COMPARISON OF 3-D TOMOGRAPHIC ALGORITHMS FOR VASCULAR RECONSTRUCTION

A. ROUGEE, K.M. HANSON[+] and D. SAINT-FELIX

THOMSON-CGR, 283 R. de la Minière, 78530 - Buc, FRANCE
[+] Los Alamos National Laboratory, MS P940, Los Alamos, New Mexico 87545, USA

ABSTRACT

We make a comparison of the performances of various three-dimensional reconstruction algorithms for situations where only few conic projections of a vascular tree are available. This problem is ill-posed and prior information must therefore be used to regularize the solution. We restrict ourselves to methods that are able to handle the sparseness and the non-negativity that caracterize a iodinated vascular structure: the Extreme Value Technique and related methods, and the Algebraic Reconstruction Technique. The results we obtained led us to derive a new method based on a two steps detection-estimation scheme.

1. INTRODUCTION

Reconstructing a three-dimensional (3-D) object from a set of its 2-D conic projections is an inverse problem which cannot be considered as an elementary extension of what is commonly done today in 2-D standard CT. The 3-D problem arises specific theoretical and computational difficulties. The inversion of the analytical relationship between a 3-D function and its divergent beam X-ray transform[1], either directly or through a transform (3-D Fourier transform, 3-D Radon transform), requires conditions on the trajectory of the source. But the sufficient conditions given in litterature[2,3,4] are unrealistic in the case of medical applications. For example, the Tuy's condition, which is the less restrictive, states that any plane that intersects the object to be reconstructed, assumed to have a finite support, must intersect the source trajectory. When these conditions cannot be verified for some practical reasons, the problem usually amounts to reconstructing with views in a limited angle. Since the Fourier's or Radon's domain are then not totally filled, the reconstruction problem becomes an ill-posed one. This characteristic is amplified by the truncation of the 2-D views which is unavoidable in medical imaging, at least in the direction of the body axis, and by the smallness of the number of views one may dispose of in some applications.

It is well known that solving such an ill-posed problem requires its regularization, i.e. the explicit introduction of a priori information on the solution in order to stabilize it. But the reconstruction methods which are based on direct inversion schemes, either exact or approximated[3,4,5,6,7], do not allow one to take into account a large variety of prior information. This explains why these direct methods fail when projections either lie in a limited angle, or are truncated. As these constraining conditions are intrinsic to the medical applications we are interested in, we shall focus here on 3-D reconstruction methods that rely on estimation schemes because they allow an easy introduction of prior information, and thus enable one to regularize the problem. But the counterpart of this flexibility is the computational load which may become excessive in a 3-D environment. Some properties of the object may however be used to easily derive "fast" algorithms and reduce the computations.

The necessity of introducing prior information on the solution implies that regularizing methods are suited to the only class of problems which correspond to the information that is used. Moreover the efficiency of these methods increases when prior information increase. Thus we restrict ourselves here to the reconstruction of a vascular tree which has been opacified by injection of a contrast medium. We assume that only few tens of conic projections are available, each projection being obtained by logarithmic substraction of images measured before and after injection of the contrast medium. The prior informations about this class of objects are positivity, sparseness, high contrast and connectivity.

Different methods have been proposed in the litterature to reconstruct a vascular tree. Besides approaches based on stereo-vision techniques, a first class of methods use assumptions on the object geometry to develop models with few parameters, and then derive fast estimation algorithms[8]. But these parametric approaches usually suffer from a high sensitivity to the exactness of the assumptions used for modelling. This can be redhibitory when actual objects, such as physiological ones, offer a geometry too complex and variable to be easily modelled with few parameters. A second class of methods relies fundamentally on the vascular trees sparseness[9,10]. The computational burden is then reduced by the crudeness of the estimation procedure. But the counterpart is a poor robustness to noise.

In this paper, we shall therefore focus on non parametric regularizing methods for reconstructing a 3-D vascular tree from few conic projections. We shall compare first the performances of existing methods: the Extreme Value Technique (EVT)[9] and related methods[10] on one hand, and the Algebraic Reconstruction Technique (ART)[11] on the other hand. The analysis of their advantages and drawbacks will lead us next to derive a reconstruction method based on a detection-estimation scheme. The detection step, based on a statistical analysis in the projections, allows one to define a region of support of the object, and thus to reduce the computational load of the estimation step. Finally, simulation results are given.

2. COMPARISON BETWEEN EXISTING METHODS

We make here a comparison of existing methods which are potentially able to reconstruct a 3-D vascular tree when only few tens of its conic projections are available. Let us introduce first some notations. We assume that the object of interest is sampled on a regular cartesian mesh, and let $f(v)$ be the value of the voxel localized in the object coordinates system by the three-components vector v. The voxels values are lexicographically concatenated into the vector f. Let $g_i(p)$ be the projection value in the ith conic projection, $i=1,...,N$, of the pixel at location defined by the two-components vector p, concatenated into the vector g_i. A projection g_i is related to the object f through the X-ray conic projection operator H_i:

$$g_i = H_i f \quad .$$
(2.1)

The location in the ith projection plane of the conic projection ray that goes through the voxel localized by v will be denoted by $p_i(v)$ and referenced as its geometrical projection. The difficulties introduced by the quantization steps in the projection planes are assumed to be solved by an appropriate interpolating scheme[12].

2.1 The Extreme Value Technique

The Extreme Value Technique (EVT)[9,10] was initially developed for tomosynthesis but its principle can be easily extended to the 3-D CT. EVT assumes that the object of interest is sparse and that, for any voxel which does not belong to the object ("empty" voxel), there exists at least one projection such that the corresponding ray passing through this voxel intersects only empty voxels. Considering the substraction projection images of a vascular tree with a positive iodine contrast, this assumption can be considered as verified if N is large enough. EVT makes an explicit use of it by assigning to $f(v)$ the minimum value of all the projections that pass through it:

$$f(v) = \text{Min } \{g_i(p_i(v)), \ i=1,...,N\} \quad .$$
(2.2)

It is obvious that EVT requires very few computations, but it is very sensitive to noise on the projections, and it misestimates the linear attenuation coefficient since the back-projected value corresponds to an integral through the object. This is a serious drawback since an object with an uniform attenuation is reconstructed with a non uniform one; any post-treatement based on a quantitative usage of the attenuation is therefore prohibited. These shortcomings will be put into light by the results presented in Section 4.

2.2 The iterative Extreme Value Technique

An iterative method has been derived from EVT by Kruger[10] to reduce the effects of noise. The basic idea is to realize a tradeoff between backprojection and EVT by defining:

$$g_k(p_i(v)) = Min \{g_i^{k-1}(p_i(v)), f^{k-1}(v)\}$$ (2.3)

$$f^k(v) = (1/N) \sum_{i=1,\ldots,N} g_i^k(p_i(v))$$ (2.4)

where k is the iteration number. This procedure converges to the EVT solution when k → ∞ but no stopping rule can be easily given. It is fruitfull[10] to replace quantities in the righthand term in (2.3) by their absolute values since the noise, and therefore $g_i(p)$, may have negative values in DSA images. If the stability of (2.3-4) is improved with respect to (2.2), the remark about the misestimation of the attenuation still stands.

2.3 The iterative threshold Extreme Value Technique

An other modification of the basic EVT has been proposed in [10] in order to improve its efficiency when projections are noisy. The projection updating equation (2.3) is replaced by:

$$g_i^k(p_i(v)) = \begin{cases} 0 & if \ g_i^{k-1}(p_i(v)).f^{k-1}(v) < 0 \\ Min \{g_i^{k-1}(p_i(v)), f^{k-1}(v)\} & otherwise \end{cases}$$ (2.5)

since negative value for $g_i(p)$ are expected in the background where noise only is present.

2.4 The Algebraic Reconstruction Technique

This well known reconstruction method[11] is based on a totally different approach. It stands on the Kaczmarz's method which iteratively computes the generalized inverse of a system of linear equations. Although this solution is unstable when the problem is ill-posed, regularization is obtained by stopping the iterations according to a given rule and by introducing prior information on the solution[13]. The ART is described by:

$$f^k = Cf^{k-1} + \lambda^k \ H_i^* \varepsilon_i^k \ / \ |H_i|^2$$ (2.6)

$$\varepsilon_i^k = g_i - H_i f^{k-1}$$ (2.7)

where C is a constraint operator describing prior information such as non-negativity:

$$Cf(v) = \begin{cases} 0 & if \ f(v) < 0 \\ f(v) & otherwise \end{cases}$$ (2.8)

ART involves heavy computations at each recursion, specially to compute the residual ε_i and to backproject it using an adequate interpolation scheme, and several iterations are required to achieve a satisfactory solution. Moreover, the sparseness assumption cannot be directly handled with the constraint formulation (2.8) since it would need to know accurately the object geometry before reconstructing. The detection step presented in the next section has been developed for this purpose.

2.5 Comparison

The performances of the above methods can be evaluated through the litterature results and, as far as our application is more specifically concerned, through our results that are grouped in Section 4 for clarity. The EVT and related methods offer a great computional

simplicity but their suffer from a poor robustness with respect to noise and to the validity of the sparseness assumption. Moreover, the misestimation of the voxel value represents a severe drawback. On the contrary, ART offers a good robustness with respect to the noise and the geometry of the projections (number, angle...), and it reconstructs an object whose X-ray projections are consistent with the available measurements. But this is achieved at the expense of a high computational burden. Considering that only few percents of the voxels belong to the object, the restriction of the estimation to these only voxels could provide great computation savings. We shall therefore develop now a detection method to determine the region of support of the object and thus to take benefit of both previous approaches.

3. DERIVATION OF A DETECTION METHOD

The goal of the detection step is the elimination of parts of the volume to be reconstructed where no object of interest is present. In this Section, we first introduce a detection method which is simply derived from the EVT, and then we present a more general framework based on statistical hypothesis testing, from which it is possible to derive various more sophisticated detection schemes.

3.1 A detection scheme based on Extreme Value

As mentioned before, the performance of EVT is very much degraded in the presence of noise. Nevertheless, the information provided may be usefull regarding the region of support of the object. Specifically, let us consider an empty voxel v, i.e. a voxel such that $f(v)=0$, and assume that there exists some views, with indices $i \in \Pi(v)$, whose corresponding projection ray intersects only empty voxels. Then we note that the measured values $g_i(p_i(v))$, which we shall denote simply by g_i, for $i \in \Pi(v)$, correspond to independent realizations of noise only. Thus, the probability that one of them is lower than the noise mean value is close to 1 if the number of indices in $\Pi(v)$, denoted by $\pi(v)$, is large enough. On the other hand, when the voxel v does belong to the object, i.e. has a non-negative value $f(v)$, each of the g_i, $i=1,...,N$ contains a non-negative term to which noise is added; thus the same probability is small in this case. Therefore, we define a decision rule as follows:

$$v \text{ is not empty} \Leftrightarrow \text{Min } \{g_i, i=1,...,N\} > m_0 \quad , \quad (3.1)$$

where m_0 is the noise mean value. Then under the assumption that the noise is symmetric, the probability of first kind error (frequency of false positive, i.e. empty v not detected empty) may be estimated simply by:

$$\text{Prob } (\text{Min } \{g_i, i=1,...,N\} > m_0) \leq \text{Prob } (\text{Min } \{g_i, i \in \Pi(v)\} > m_0) \leq (1/2)^{\pi(v)} \quad , \quad (3.2)$$

whereas the probability of second kind error (frequency of false negative, i.e. non-empty voxel v detected empty) depends on the actual but unknown probability law of the g_i. This provides us with a simple detection scheme with low computational cost.

This detection method makes use of prior knowledge on the object (non-negativity, sparseness) and the noise, and of the assumption on the existence of separating views. Moreover, some drawbacks inherent to the EVT are removed since the attenuation value is not of interest here, and over-estimation of the region of support is not redhibitory. Nevertheless, this technique is still very primary, and fails to detect small vessels since it is very sensitive to the noise: when increasing the number of views, small parts of the object are more likely to be lost, since low realizations of the noise are more likely to occur, whereas, when decreasing the number of views, the separating views assumption becomes no more valid for a given object complexity, and structure artifacts may appear between differents parts of the object. A better compromise between first and second kind detection errors has to be established, and this lead us to consider more sophisticated detection schemes.

3.2 A more general framework for detection

Let us now consider, for a given voxel $\mathbf{v}$ and in each view i, a "projection window" denoted by PW_i, of size K by K (K odd), centered on the geometric projection of the voxel. Let us assume that within each window PW_i the measured pixels values denoted by $g_i^{m,n}$, $m,n=1,\ldots,K$ are K^2 observations of a random variable P_i with mean m_i and standard deviation σ_i. In practice, this means that the noise is assumed stationary and white. The detection problem may then be formulated as follows: test $H_0=\{\mathbf{v}$ is empty$\}$ against $H_1=\{\mathbf{v}$ has a non-negative density$\}$, given the $g_i^{m,n}$, $m,n=1,\ldots,K$ and $i=1,\ldots,N$.

In a first step, we consider separately each view i, and we define the following hypothesis testing problem: test $H_{0,i}=\{m_i=m_0\}$ against $H_{1,i}=\{m_i>m_0\}$, where m_0 is the noise mean value. This is nothing else than a one-sided test on the mean of the random variable P_i. Let $\hat{m}_i$ denote the mean estimator for the variable P_i, and $\hat{\sigma}_i^2$ the variance estimator:

$$\hat{m}_i = 1/K^2 \sum_{m,n=1,\ldots,K} g_i^{m,n} \quad , \tag{3.3}$$

$$\hat{\sigma}_i^2 = 1/(K^2-1) \sum_{m,n=1,\ldots,K} (g_i^{m,n} - \hat{m}_i)^2 \quad . \tag{3.4}$$

The test may be implemented with the following statistics:

$$Z_i = (\hat{m}_i - m_0) / \sqrt{\hat{\sigma}_i^2 / K^2} \quad , \tag{3.5}$$

where $\hat{\sigma}_i$ may be replaced by σ_i if σ_i is known. More precisely, under the assumption that the $g_i^{m,n}$ are independent and that P_i is gaussian, the statistics Z_i follows a Student distribution with K^2-1 degrees of freedom (or a gaussian distribution with standard deviation 1 if σ_i is known), centered under $H_{0,i}$, whereas under $H_{1,i}$ its non-centrality parameter is:

$$\delta_i = (m_i - m_0) / (\sigma_i / K) \quad . \tag{3.6}$$

The hypothesis $H_{0,i}$ is then rejected at level α on the region defined by $\{Z_i>t_\alpha\}$, where the threshold t_α is chosen such that its probability under $H_{0,i}$, i.e. the first kind error, is lower or equal to the desired level α, and the second kind error may be calculated with respect to the parameters m_i, σ_i and t_α.

Going back to our detection problem, we remark that, making explicit use of the assumption on the existence of separating views, H_0 is equivalent to say "there exists at least one view i in which $H_{0,i}$ is true" i.e. H_0 is equivalent to the union of the $H_{0,i}$, $i=1,\ldots,N$. Having defined a region of rejection of $H_{0,i}$ at level α by $\{Z_i>t_\alpha\}$ for each $i=1,\ldots,N$, a solution to our problem is simply to choose the following decision rule:

$$\mathbf{v} \text{ is not empty} \Leftrightarrow Z = \text{Min} \{Z_i, i=1,\ldots,N\} > t_\alpha \quad , \tag{3.7}$$

which corresponds to a region of rejection of H_0 equal to $\{Z>t_\alpha\}= \cap_{i=1,\ldots,N}\{Z_i>t_\alpha\}$. Furthermore, the first kind error which may be estimated by:

$$P_0 (Z > t_\alpha) \le P_0 (\text{Min} \{Z_i, i\in\Pi(\mathbf{v})\} > t_\alpha) = \alpha^{\Pi(\mathbf{v})} \quad , \tag{3.8}$$

is much smaller than the expression in (3.2) for usual values of the level α (about 0.1).

Let us note that this procedure does not result in a global testing of the hypotheses $\{H_{0,i}, i=1,\ldots,N\}$, since a voxel is rejected from the region of support (i.e. H_0 accepted) according to the pixel values in only one view, in fact the "most separating" view. Nevertheless, the introduction of projection windows considerably improves the robustness with respect to the noise and thus the performances of the detection. Furthermore, the testing statistics introduced in (3.5) are normalized, contrary to the EVT used previously,

so that they are suited to our detection problem as it was formulated, and that in practice the threshold is easier to determine with respect to the tolerated detection errors.

3.3 Discussion

The introduction of a more general statistical framework for detecting a region of support of the object to be reconstructed provides us with a more versatile tool, which is more robust with respect to the uncertainties on the signal. The hypothesis made on the noise within the projection windows (stationary, white and gaussian) may seem at first unrealistic, but one way to overcome this problem is to implement a preliminary whitening of the data. Let us note that the use of a priori knowledge in this framework is of great importance, and has been introduced through parameters such as the noise statistics, number and size of projection windows and possibly type of neighbourhood used in the preliminary smoothing, and through the use of the separating views assumption.

4. SIMULATION RESULTS

All the presented simulation results were obtained with a synthetically generated vascular tree, with uniform density 1, stored in a 64^3 volume. This object is rather realistic and presents a reasonable complexity, as one may see on the three dimensional view of its surface (Figure 1.a), and on the two horizontal slices represented in Figures 1.c-1.d. A set of 15 conic projections of size 64^2 was generated using an interpolation on functions basis, corresponding to a circular trajectory of the X-ray source around a vertical axis. Figure 1.b shows one of these projections after addition of a centered gaussian noise with standard deviation 0.5, corresponding to a SNR equal to 20 dB.

In Figures 2-3 some results obtained with the EVTs are represented for the two selected slices, simultaneously and with the original slices for comparison. One may remark that, even in the noiseless case, the standard EVT defined in (2.2) fails to reconstruct concave parts of the object (Figure 2.b) and misestimates the density values which leads to mismatching of small vessels (Figure 2'.b), and that this method is very sensitive to the noise (Figures 2.c-2'.c). Nevertheless, after introduction a non-negativity constraint in this technique, most of the noise artifacts in the background are removed (Figures 2.d-2'.d). The three iterative versions introduced in[10] produce also a reduction of the noise artifacts but in a much softer way (Figures 3-3'). Moreover, the benefits of the introduction of a non-negativity constraint in the third version defined in (2.3), (2.5) seem to be canceled by the use of an iterative scheme (Figures 3.d-3'.d).

The results presented in Figure 4 were obtained using 4 iterations of ART with a non-negativity constraint. Although the computation time is much larger with this technique, these results are considerably more satisfactory. A good estimation of the object morphology is obtained using either noiseless or noisy projections, for concave parts (Figures 4.a-4.c) as well as for small parts of the object (Figures 4.b-4.d), and the backprojection artifacts are not of great annoyance even in the noisy case (Figures 4.c-4.d).

The detection scheme (3.1) derived from EVT produces fairly good results, with only 2.7% of voxels lost (relative to the number of voxels in the original vascular tree), mainly situated in very small vessels, and 3.4% of false alarms (relative to the number of empty voxels in the original volume), mainly spread over the volume (Figure 5.a-5.b). When increasing the value of the threshold m_0 from 0. to 1. in order to remove the background artifacts, the global relative amount of false alarms lowers down to 0.7%, whereas the relative amount of voxels lost is raised up to 18%. One may note that even large vessels then present missing voxels (Figure 5.c), and most of the small vessels are totally mismatched (Figure 5.d) which is not acceptable.

The region of support obtained with the detection algorithm based on the Student

statistics (3.5), shown in Figures 6.a-6.b, for t_α=2.575 which corresponds to a theoretical level for each view α=5%, presents only 2.2% of voxels lost and 4.5% of false alarms, mostly distributed around the object, producing an overestimation of its region of support, with a background cleared of all the noise artifacts. When increasing the threshold t_α up to 10. in order to better separate the different vessels of the tree, many small vessels and also parts of larger vessels are lost (Figures 6.c-6.d).

Comparing the frequency distributions of the EVT statistics and the Student statistics on the two sets of empty and non-empty voxels (Figures 7-8), one may check that in both cases the two distributions overlap, but in Figure 8 the distribution of the Student statistics is narrower and higher on the empty voxels, and more spread out on the non-empty voxels, which indicates that it better characterizes the noise and signal behaviours.

Finally, a reduction of the noise artifacts and of the global computational cost (number of parameters to be estimated, and number of iterations needed) is observed after restriction of the estimation algorithm to the region of support provided by the detection algorithm. As one may check in Figure 9, the quality of the reconstruction obtained after only 1 iteration of constrained ART, using the region of support detected with the EV statistics (Figures 9.a-9.b) or the Student statistics (Figures 9.c-9.d) is similar to the one after 4 iterations in Figure 4, although some false alarms artifacts are not yet eliminated specially in 9.b.

5. CONCLUSION

The comparison of the performances of three-dimensional reconstruction algorithms for a vascular tree from few conic projections shows that a regularized solution to this ill-posed problem may be obtained by introducing prior information. This is well achieved by the procedure we introduced, consisting in a statistical detection step and an estimation step based on the Algebraic Reconstruction Technique, as we have shown in our simulation results.

6. REFERENCES

1. D.V. Finch, D.C. Solmon, "A characterization of the range of the divergent beam X-ray transform," SIAM J. Math. Anal., 14, 767-771 (1976).
2. A.A. Kirillov, "On a problem of I.M. Gel'fand," Soviet. Math. Dokl., 2, 268-269 (1961).
3. H.K. Tuy, "An inversion formula for cone-beam reconstruction," SIAM J. Appl. Math., 43, 546-552 (1983).
4. B.D. Smith, "Image reconstruction from cone-beam projections: necessary and sufficient conditions and reconstruction methods", IEEE Trans., MI-4, 154-25 (1985).
5. P. Grangeat, Analyse d'un système d'imagerie 3-D par reconstruction à partir de radiographies X en géométrie conique, Thesis, ENST, Paris, (1987).
6. L.A. Feldkamp, L.C. Davis, and J.W. Kress, "Practical cone-beam algorithm," J. Opt. Soc. Am., 1(6), 612-619 (1984).
7. D.V. Finch, "Cone beam reconstruction with sources on a curve," SIAM J. Appl. Math., 45, 665-673 (1985).
8. Y. Bresler, A. Macovski, "3-D reconstruction from projections with incomplete and noisy data by object estimation," IEEE Trans., ASSP-35, 1139-1153 (1987).
9. P. Haaker, E. Klotz, R. Koppe, R. Linde, and H. Moller, "A new digital tomosynthesis method with less artifacts for angiography," Med. Phys., 12, 431-436 (1985).
10. R.A. Kruger, D.R. Reinecke, S.W. Smith, and R. Ning, "Reconstruction of blood vessels from x-ray substraction projections: limited angle geometry," to appear in Med. Phys. (1987).
11. R. Gordon, R. Bender, and G.T. Herman, "Algebraic reconstruction technique for three-dimensional electron microscopy and X-ray photography," J. Theo. Biol., 29, 471-481 (1970).
12. K.M. Hanson and G.W. Wecksung, "Local basis-function approach to computed tomography," Appl. Opt., 24(23), 4028-4039 (1985).
13. D. Saint-Félix, Restauration d'image: régularisation d'un problème mal-posé et algorithmique associée, Thèse de Doctorat es-Sciences, Univ. de Paris-Sud, (1987).
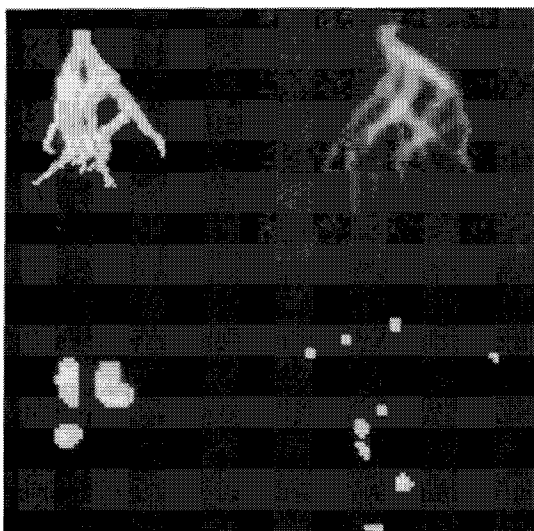
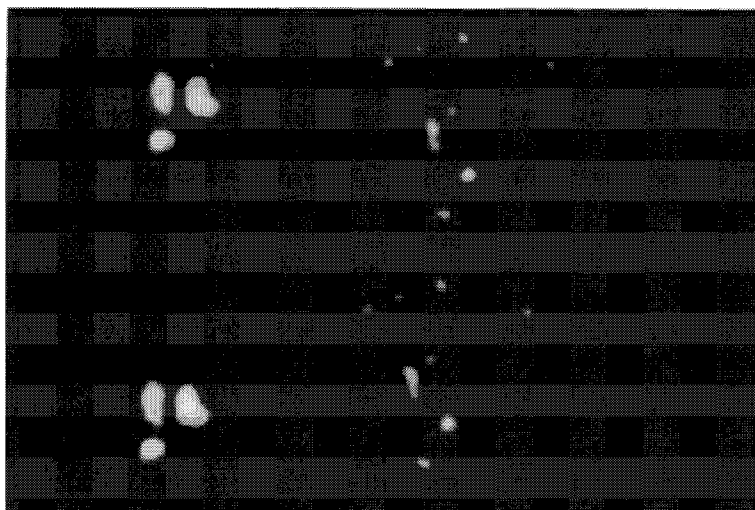Fig. 1: Original object 3-D display (a), noisy projection (b), two planes (c-d).

Fig. 4: Noiseless constrained ART (a-b), noisy constrained ART (c-d), 4 iterations.
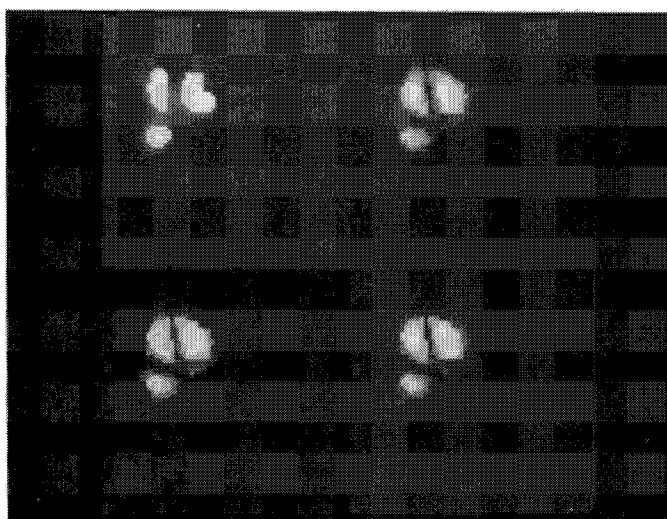

Fig. 2: Original (a), noiseless EVT (b), noisy EVT (c), noisy constrained EVT (d).
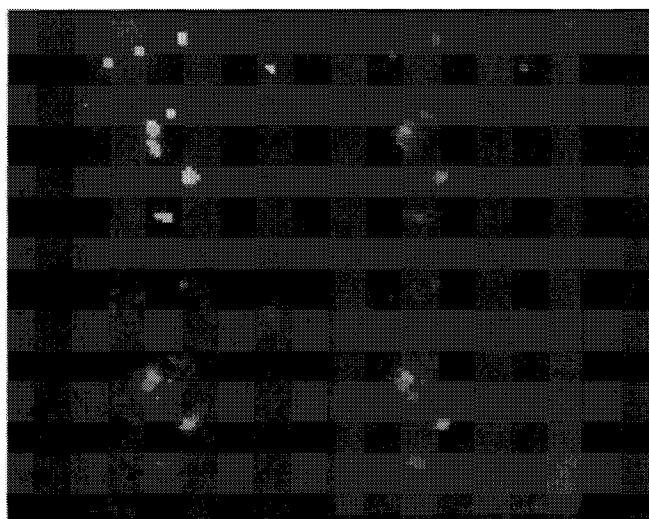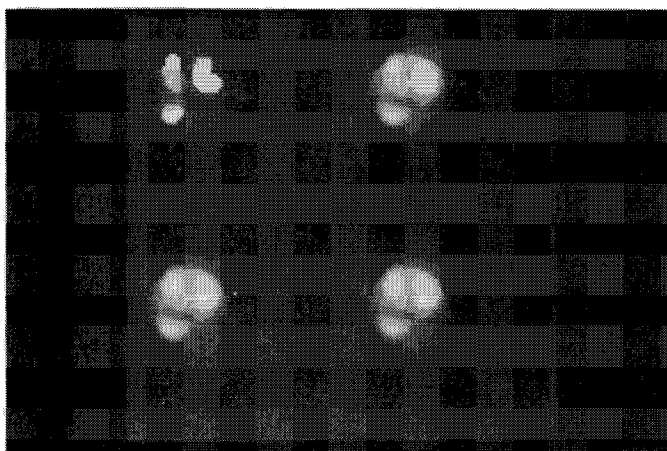

Fig. 2': Same as Fig. 2.

Fig. 3: Original (a), iterative EVT (b), with absolute value (c), and threshold (d).
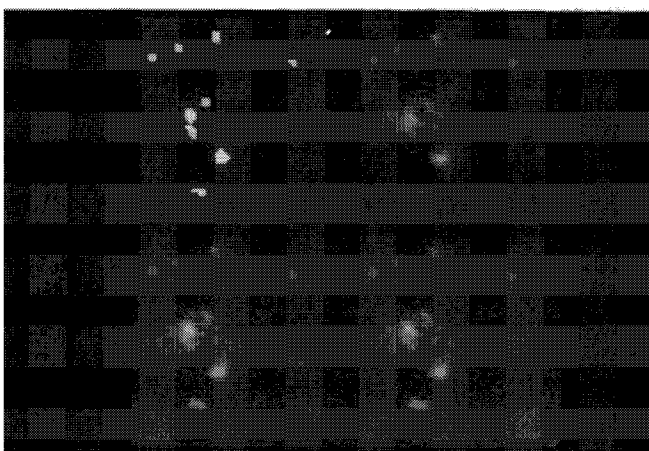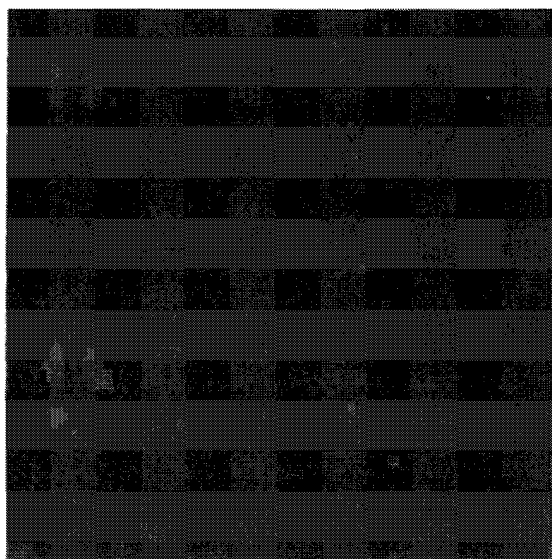

Fig. 3': Same as Fig. 3.

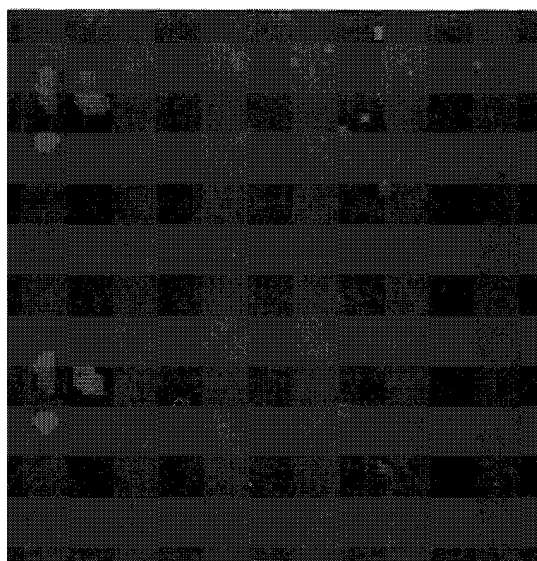Fig. 5: Region of support detected by EVT, $m_0=0$. (a–b), and $m_0=1$. (c–d).

Fig. 6: Region of support detected by Student, $t_\alpha=2.575$ (a–b), and $t_\alpha=10$. (c–d).

(black= true neg., white= true pos., light grey= false pos., dark grey= false neg.)
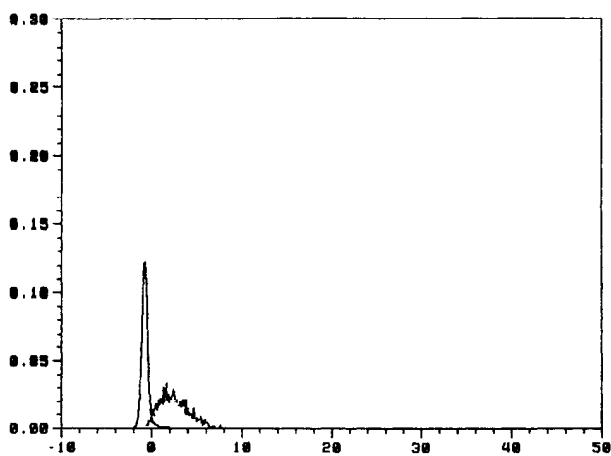

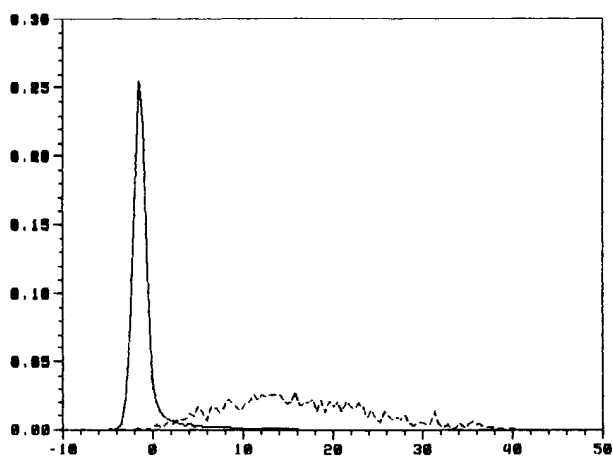Fig. 7: Histograms of EVT on empty (solid line) or non-empty voxels (dashed line).

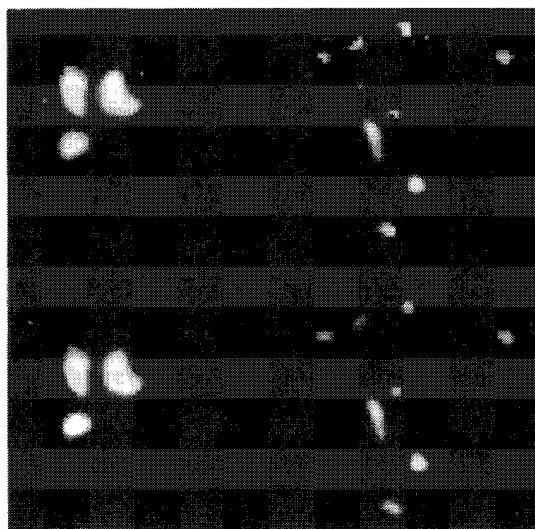

Fig. 8: Same as Fig. 7 for Student.

Fig. 9: ART with region of support detected by EVT (a–b) or Student (c–d), 1 iteration.